Research Article

Charge detection mass spectrometry of bacteriophage P22 procapsid distributions above 20 MDa

David Z. Keifer[1], Elizabeth E. Pierson[1], Joanna A. Hogan[1], Gregory J. Bedwell[2], Peter E. Prevelige[2] and Martin F. Jarrold[1]*

[1]Department of Chemistry, Indiana University Bloomington, Bloomington, IN 47405, USA
[2]Department of Microbiology, University of Alabama at Birmingham, Birmingham, AL 35294, USA

RATIONALE: Charge state resolution is required to determine the masses of ions in electrospray mass spectrometry, a feat which becomes increasingly difficult as the mass increases. Charge detection mass spectrometry (CDMS) circumvents this limitation by simultaneously measuring the charge and the m/z of individual ions. In this work, we have used electrospray CDMS to determine the number of scaffolding proteins associated with bacteriophage P22 procapsids.
METHODS: P22 procapsids containing a native cargo of scaffolding protein were assembled in *E. coli* and purified via differential centrifugation. Electrospray CDMS was used to measure their mass distribution.
RESULTS: The procapsid peak was centered at 23.60 MDa, which indicates that they contain an average of ~112 scaffolding proteins. The distribution is relatively narrow, less than 31 scaffolding proteins wide. In addition, a peak at 19.84 MDa with a relative abundance of ~15% is attributed to empty capsids. Despite having the same sizes in solution, the empty capsid and the procapsid have significantly different average charges.
CONCLUSIONS: The detection of empty capsids is unexpected and the process that leads to them is unknown. The average charge on the empty capsids is significantly lower than expected from the charge residue model, which probably indicates that the empty capsids have contracted in the gas phase. The scaffolding protein presumably limits the contraction of the procapsids. This work shows that electrospray CDMS can provide valuable information for masses greater than 20 MDa. Copyright © 2014 John Wiley & Sons, Ltd.

Ever-growing interest in viruses from the standpoint of materials and medicinal science has led to the development of analytical techniques suitable for the characterization of viral components. Electrospray mass spectrometry, in particular, has proven to be a useful tool for the analysis of intact biomolecules in the gas phase and therefore has been used to study viral genomes[1] and viral structural proteins and dynamics.[2–6] The study of intact virus capsids, for a time, remained unattainable because of difficulty transmitting and detecting particles in the MDa mass regime. Specifically, most electrosprayed virus particles have mass-to-charge ratios (m/z) in the tens of kTh range (where 1 kTh = 1000 Da/z), which is beyond the m/z range of most commercial mass spectrometers. In addition, these massive, slow-moving particles are not detected efficiently on conventional microchannel plate detectors.[7] Finally, high charge states along with mass heterogeneity prevent m/z charge state resolution that is critical for mass determination. Despite these hindrances, in 2000, Tito *et al.* demonstrated that it was possible to detect the ~2.5 MDa bacteriophage MS2 capsid on a time-of-flight (TOF) mass spectrometer, though the m/z spectrum lacked charge state resolution due to a number of chemical and instrumental factors.[8] Subsequent efforts by Uetrecht *et al.* have led to the detection of 3 and 4 MDa hepatitis B virus (HBV) capsids with sufficient charge state resolution to determine the mass of the protein shells to within 0.1%.[9] Most recently, Snijder *et al.* used a modified quadrupole TOF (QTOF) tandem mass spectrometer to determine the mass of the ~18 MDa capsid from bacteriophage HK97.[10] Though significant progress has been made over the past decade, the study of intact virus capsids with conventional electrospray mass spectrometry methods is still limited to highly homogeneous samples with known masses due to insufficient charge state resolution in the m/z spectrum.

Charge detection mass spectrometry (CDMS) is an alternative method for measuring the masses of ions in the kDa and MDa mass regime that circumvents the ongoing issue of m/z charge state resolution.[11–16] The mass analyzer consists of a conductive charge detection cylinder that is capable of simultaneously measuring the charge (z) and m/z of a single electrosprayed ion. The CDMS design by Fuerstenau and Benner[11] was successful in measuring a 1.66 MDa viral genome[13] as well as intact rice yellow mottle virus (~6.5 MDa) and tobacco mosaic virus (~40.5 MDa).[16] Though accurate, the reported masses had poor precision mainly due to the uncertainty in the charge measurement (~75 charges). In addition, a lower limit of charge detection

---

* *Correspondence to:* M. F. Jarrold, Department of Chemistry, Indiana University Bloomington, Bloomington, IN 47405, USA.
E-mail: mfj@indiana.edu

Rapid Commun. Mass Spectrom. **2014**, *28*, 483–488

Copyright © 2014 John Wiley & Sons, Ltd.

483

of 250 charges prevented the technique from becoming more widely used, as most species carry less charge when transferred into the gas phase.

Recent work in our laboratory has focused on improving the CDMS method.[17–19] Improvements include the use of a modified cone trap[20] to provide long trapping times, energy analysis of the ions before they enter the trap, a liquid-nitrogen-cooled JFET at the input of the charge-sensitive preamplifier, random sampling of the ions which allows lower charges to be detected, and the use of a fast Fourier transform to analyze the signals from the image charge detector. With these modifications, we have achieved a charge accuracy of 0.7 charges and a limit of detection of 6 charges. The uncertainty in the m/z measurement (~1% RMSD) ultimately limits the instrumental mass resolving power ($m/\Delta m$) to ~40 (FWHM) in the studies reported here.

Using CDMS, we have measured the mass distribution of $T = 7$ procapsids from the bacteriophage P22, a particle weighing more than 20 MDa. *In vivo*, P22 coat proteins assemble into procapsids that encapsidate a number of scaffolding proteins that catalyze the assembly of procapsids with the correct morphology.[21] During DNA packaging, the inner shell of the scaffolding protein dissociates and exits the procapsid. We have measured the masses of both the empty shells (19.84 MDa) and the procapsids containing a distribution of scaffolding proteins (23.60 MDa). The mass measurement of the latter peak indicates that, on average, 112 scaffolding proteins were encapsidated with a distribution that was less than 31 scaffolding proteins wide (FWHM). The measurement of a heterogeneous population of species in the 20 MDa mass regime represents an important milestone in virus mass spectrometry as previous experiments were limited to homogenous samples.

EXPERIMENTAL

P22 capsid assembly, purification, and TEM imaging

Procapsids were produced under a T7-driven over-expression system in ampicillin BL21-DE3 *E. coli* grown in LB media. The plasmid used was a pET-3a derived plasmid containing P22 genes *5* (coat protein, 46,621 Da[22]) and *8* (scaffolding protein, 33,565 Da[22]) expressed in tandem. Protein expression was induced at mid-log phase with 0.5 mM isopropyl β-D-1-thiogalactopyranoside (IPTG). Four hours after induction, cells were pelleted at 7000 *g* and resuspended in 10 mL Buffer B (50 mM Tris-Cl, pH 7.6, 25 mM NaCl)/1 L culture. Cell lysis was achieved by repeated freeze-thaw cycles, followed by sonication to shear nucleic acid and reduce the viscosity of the solution. Cell debris was pelleted at 27 000 *g* for 45 min, and the supernatant was layered on top of a 20% sucrose cushion. The procapsids and other larger, soluble cellular components were pelleted through the sucrose cushion by centrifugation at 311 000 *g* for 2 h. The pelleted material was resuspended in 20 mL of Buffer B and pelleted at 311 000 *g* for 1 h to remove residual sucrose. The pellet was resuspended in 500 µL of Buffer B and layered on top of a 5–20% sucrose gradient. The gradient was centrifuged at 200 000 *g* for 35 min. The procapsid band, apparent by turbidity, was removed by puncturing the tube and removal

of the band with a syringe. The purified procapsid sample was then dialyzed against Buffer B to remove sucrose. For concentration and buffer exchange for mass spectrometry, the procapsid sample was pelleted and resuspended in 25 mM ammonium acetate.

In order to confirm that P22 capsids persist in 25 mM ammonium acetate, negative stain transmission electron microscopy (TEM) was performed on *in vitro* procapsids prepared by incubating excess wild-type scaffolding protein with 20 µM empty shells overnight at 4 °C. The reentry products were pelleted, separating stuffed shells from scaffolding monomers, and resuspended in 25 mM ammonium acetate. Grids for TEM were prepared by adding 4 µL of the procapsid solution to a copper grid. The sample was allowed to sit on the copper grid for 4 min before several washes with water were performed. After sufficient washing, 4 µL of a 2% uranyl acetate solution was added to the grid and let sit for an additional 4 min before blotting. The dried grid was imaged in an FEI Tecnai 12 with an acceleration voltage of 80 kV and a spot size of 3. Images were collected at a magnification of 42 000×. A representative micrograph is shown in Fig. 1; the scale bar is 100 nm. The abundant presence of complete capsids demonstrates the persistence of P22 capsids in 25 mM ammonium acetate.

Charge detection mass spectrometer

Our home-built charge detection mass spectrometer has been described elsewhere.[17–19] Ions were generated by nano-electrospray with a 25 mM ammonium acetate (99.99%, Sigma-Aldrich) solution in HPLC-grade water (OmniSolv, EMD Millipore) containing ~1 mg/mL total protein. The ions are entrained in a flow of the background gas that carries them through a heated capillary and into the first differentially pumped region, which contains an ion funnel. The ions are transported through the second and third differentially pumped regions containing a hexapole and a quadrupole, respectively, and then pass into the final differentially pumped region. The resulting ion beam is
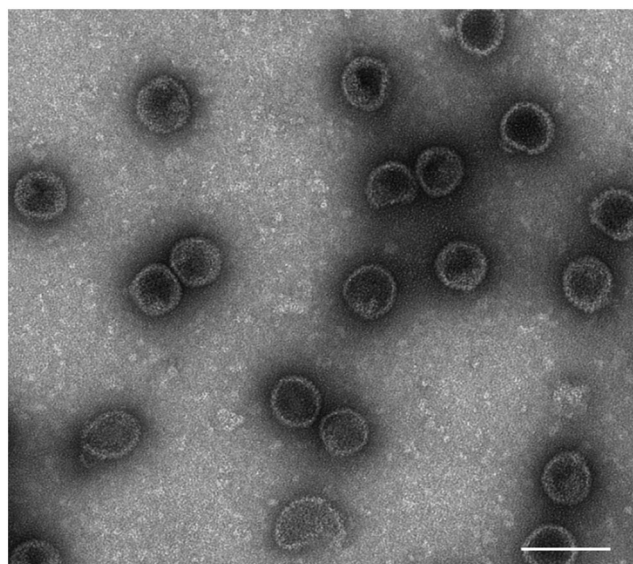
Figure 1. Negative-stain TEM micrograph of P22 procapsids in 25 mM ammonium acetate. Scale bar is 100 nm.

focused with an asymmetric einzel lens either into the extraction region of an orthogonal acceleration time-of-flight mass spectrometer or into another einzel lens at the entrance of a dual hemispherical deflection analyzer (HDA). Only ions within a narrow range of kinetic energies per z, centered at 100 eV/z, are transmitted through the dual HDA. The transmitted ions are passed into a modified cone trap containing a central charge detector tube. When the end caps of the trap are grounded, ions fly through the trap and impinge on a pair of MCPs in the chevron configuration that are used to monitor the signal.

To trap an ion, the end cap at the back of the trap is raised to 135 V. A short time later, the front end cap is raised to 135 V as well. Any ions within the trap at this time will not have enough energy to escape the trap and will instead oscillate back and forth between the end caps. After 95 ms of trapping, both end caps are grounded to empty the trap, and the process is repeated to trap a new ion. With each oscillation of a trapped ion, an image charge proportional to the ion's z is imprinted on the charge detector tube in the center of the trap. The image charge is detected by a liquid-nitrogen-cooled JFET (2SK152) at the input of a charge-sensitive preamplifier (Amptek 250). A Fortran program performs a fast Fourier transform on the raw signal, producing a series of peaks in the magnitude-mode frequency spectrum that correspond to the fundamental frequency and harmonics of the ion oscillating in the trap. Simion simulations provide the following relationship between an ion's m/z and its oscillation frequency in the trap.

$$\frac{m}{z} = \frac{C}{f^2} \tag{1}$$

where f is frequency and C is a constant depending on the ion's kinetic energy per z, the voltage applied to the end caps, and the geometry of the trap. The constant C, the calibration factor that relates the measured oscillation frequency to the ion's m/z, is determined from Simion simulations. The magnitude of the ion's fundamental peak in the Fourier transform is proportional to z and to the time the ion is trapped. To calibrate the charge detection circuit, a waveform generator was used to apply signals of various known voltages, frequencies, and durations across a capacitor chain leading to the input of the JFET. The known capacitance of the capacitor chain and the voltage of the generated signal can be multiplied to give the charge passed to the input of the JFET which is usually on the order of thousands of electrons. Comparing the magnitude of the fundamental frequency peak produced by performing a fast Fourier transform on this simulated signal to the known input charge provides the z calibration. Multiplying the m/z and z of each ion yields m. The m values are then binned to provide the m spectrum. To reduce the likelihood of false-positives and to improve accuracy, only ions trapped for the full 95 ms contribute to spectra reported here.

RESULTS

P22 forms $T = 7$ capsids consisting of 420 copies of the coat protein with a theoretical average mass of 19.58082 MDa. Experiments in which the scaffolding protein was extracted

from P22 procapsids via 0.5 M guanidine hydrochloride demonstrate that our charge detection mass spectrometer measures empty P22 capsids at 19.8 MDa, which is approximately 1% higher than expected from the sequence mass. Some of this overestimation is almost certainly due to small inaccuracies in the calibration of the m/z and z measurements (see above) because we have seen similar shifts for other species we have measured. However, adducted salt ions and incomplete desolvation may also contribute to the shift. An m spectrum measured for P22 procapsids with scaffolding proteins is shown in Fig. 2. The smaller peak centered at 19.84 MDa corresponds very closely to the mass of empty P22 capsids. Thus, a fraction (around 15%) of the particles has either lost its scaffolding protein cargo or was assembled without it. The presence of this subpopulation would not be detectable by biochemical techniques which report only an average mass or composition. The larger peak centered at 23.60 MDa in Fig. 2 is due to the procapsid with scaffolding protein. The mass difference between the peak attributed to empty capsids and the one with scaffolding proteins (3.76 MDa) corresponds to approximately 112 scaffolding proteins.

With the 95 ms trapping time used here, the uncertainty in the charge determination is approximately 1.5 e (RMSD). The uncertainty in the m/z determination is ~1% (RMSD). Knowing the charge, the instrumental mass resolution (Δm) can be calculated. The width of the peak at 23.60 MDa is ~1.2 MDa (FWHM). For a single species at this mass, our instrumental mass resolution is expected to result in a peak width of 0.58 MDa (FWHM). The extra width probably results from a distribution of scaffolding protein. Assuming that the additional width is entirely due to this cause and that the distribution is Gaussian, then its width can be estimated to be approximately 31 scaffolding proteins (FWHM).

The peak centered at 19.84 MDa is narrower than the peak at 23.60 MDa but is still wider than expected from our instrumental mass resolution; there are also high and low
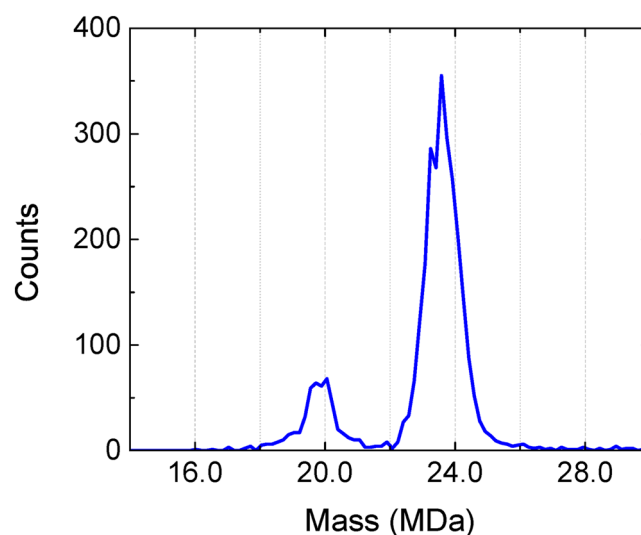
Figure 2. Mass spectrum of P22 procapsids. The measured masses are binned into a histogram with bin size 167825 Da (the mass of five scaffolding proteins). The procapsid peak is centered at 23.60 MDa. In addition there is a smaller peak centered at 19.84 MDa which is attributed to empty capsids.

mass tails on this peak. The high mass tail could come from some residual scaffolding proteins. The low mass tail extends down to below 18 MDa. This must result from capsids with fewer than the full complement of 420 coat proteins. The P22 capsid is known to lose pentamers when heated,[23] but it is not clear that missing pentamers are responsible for the low mass tail. The fact that the peak attributed to the empty capsid is broader than expected from the experimental mass resolution raises a question about whether other factors, in addition to the experimental mass resolution and the width of the scaffolding protein distribution, contribute to the width of the peak at 23.60 MDa. Thus, the FWHM of 31 scaffolding proteins mentioned above should be considered an upper limit. Even at 31 scaffolding proteins, the distribution is quite narrow.

Figure 3 is a scatter plot of *z* versus *m*, where each point represents one ion measured in the charge detection mass spectrometer. The two clusters of points correspond to empty P22 capsids and P22 procapsids. Charges on the empty capsids range from ~290 to ~360 e, centered at 325 e; procapsid charges range from ~390 to ~464 e, centered at 427 e.

DISCUSSION

The procapsid peak at 23.60 MDa in the *m* spectrum in Fig. 2 occurs at around 61 kTh in the *m/z* spectrum. Perhaps the most impressive measurement to date at a comparable *m/z* range with conventional mass spectrometry (i.e. mass spectrometry which produces *m/z* spectra from an ensemble of ions) is the mass determination of intact HK97 capsids at nearly 18 MDa by Snijder *et al*. A QTOF mass spectrometer, equipped with a collision cell to improve desolvation, was used.[10] While this was a remarkable and unprecedented achievement, just a single species was present, and charge state resolution was only incipient, presumably because of
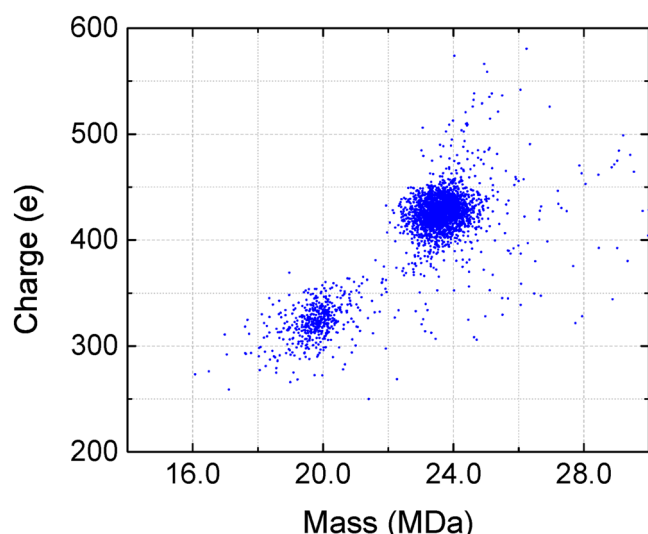
salt adducts and incomplete desolvation. With the same *m/z* peak widths it would not be possible to resolve charge states for a P22 procapsid containing exactly 112 scaffolding proteins. A realistic distribution of scaffolding proteins would create many more peaks in the same *m/z* range, further convoluting the spectrum. Therefore, the mass distribution represented by Fig. 2 could not have been determined with conventional mass spectrometry, at least not with the current technology. CDMS can accomplish the feat because it does not require charge state resolution since each ion's mass is determined individually.

Previous studies have found that the amount of scaffolding protein encapsidated in P22 procapsids depends on the relative concentrations of coat protein and scaffolding protein in the assembly solution and ranges anywhere from 50 to 300 scaffolding proteins per procapsid.[24] The methods used to determine that range were sodium dodecyl sulfate polyacrylamide gel electrophoresis (SDS-PAGE)[21,25] and cryo-electron microscopy (cryo-EM).[24] In SDS-PAGE, an ensemble of procapsids is disassembled, the proteins are denatured, and the entire sample is dispersed elect-rophoretically. The method is consequently able to determine an average number of scaffolding proteins per procapsid, but it is incapable of providing a distribution. In cryo-EM, many particles are averaged together to generate high signal-to-noise ratio images. This allows possible binding sites for scaffolding protein on the coat protein shell to be elucidated, but it precludes a distribution from being measured with this technique. A benefit of CDMS over these methods is that it provides both an average number of scaffolding proteins per procapsid and a distribution. We measured an average number of 112 scaffolding proteins which falls within the expected range, and the width of the distribution (≤31 scaffolding proteins FWHM) which was previously unknown.

Another piece of information obtained here that is not accessible by ensemble biochemical measurements is the observation that around 15% of the capsids do not carry scaffolding protein. Either a fraction of the procapsids loses its scaffolding at some point, or a fraction was initially assembled without any scaffolding. The process by which this occurs is unknown.

Both the empty capsids and the procapsids are roughly spherical and have an outer radius of approximately 28 nm, as determined previously by cryo-EM.[24] Because of their large size and compact shape, they are expected to be ionized by the charge residue mechanism.[26] According to this mechanism, an analyte remains in the electrospray droplet until the droplet evaporates, leaving the leftover charge on the analyte. Consequently, the maximum charge that the analyte ion can hold is the maximum charge that a water droplet of the same radius can hold, the Rayleigh limit, which is given by:[27]

$$ez_R = q_R = 8\pi\sqrt{\gamma\varepsilon_0 R_i^3} \qquad (2)$$

where R_i is the droplet radius, γ is the surface tension, e is the elementary charge, z_R is the maximum number of elementary charges, and ε_0 is vacuum permittivity. In practice, the ions usually become charged to between 70% and 85% of this limit.[19,27] Experimentally, this limit is independent of the

Figure 3. Charge versus mass scatter plot for all the ions in Fig. 2. The charge is in units of elementary charge (e). The empty capsids' charge distribution is centered at 325 charges and the procapsids' charge distribution is centered at 427 charges.

analyte chemical identity as the model predicts, although studies of the charge residue mechanism have mostly been limited to globular proteins.[28,29] The proposed rationalization for the independence comes from molecular dynamics simulations which show that any charge on the surface of or even in the interior of the solution-phase protein or assembly contributes to the maximum charge allowed on a stable droplet.[26]

The charge residue model would predict that the empty capsids and the procapsids have similar charge distributions since both morphologies have the same radius; however, Fig. 3 reveals that the charge distributions of these two morphologies do not even overlap. The limit obtained from Eqn. (2) for the empty capsid and procapsid is approximately 590 charges; 70–85% of this value is 410–500 charges. The average charge on the procapsids lies within this range, but the charge on the empty capsids is lower than expected. This may indicate a breakdown of the charge residue model. Another possible explanation (and probably the more likely explanation) is that the reduced charge on the empty capsids is a consequence of them contracting to more compact structures as they become desolvated and make the transition into the gas phase. This contraction has been observed for globular proteins with low charge states.[30] A decrease in the radius from 28 nm to 23 nm would bring the charges on the empty capsid in line with those on the procapsid. The scaffolding protein presumably prevents this putative contraction from occurring to the same extent in the procapsids.

CONCLUSIONS

Charge detection mass spectrometry was used to determine the mass distribution of P22 procapsids. The roughly Gaussian-shaped distribution of the procapsids was centered at 23.60 MDa, corresponding to an average of 112 scaffolding proteins. Mass peaks corresponding to specific numbers of scaffolding proteins were not resolved, but the distribution was less than or equal to 31 scaffolding proteins wide (FWHM). Unexpectedly, about 15% of the ions detected were empty P22 capsids measured at 19.84 MDa. The process that leads to these empty capsids is unknown.

Another surprise was revealed in the charge distributions of the empty capsids and the procapsids. In particular, the two charge distributions do not overlap, despite both solution-phase morphologies having the same outer radius. Either the charge residue model, the charging model most likely to explain the charging mechanism of icosahedral virus capsids, does not provide a complete description of capsid charging in electrospray, or, more likely, the empty capsids have contracted during their transition into the gas phase.

The procapsid mass distribution discussed here represents a measurement of a distribution of multiple species above 20 MDa which overlap in m/z. Even with the most impressive m/z resolution ever obtained by conventional MS in this mass range, there would be no charge state resolution, and no mass determinations could have been made. Since CDMS does not rely on charge state resolution, it is uniquely equipped to analyze mixtures of species at masses beyond what can presently be achieved with conventional MS.

REFERENCES

[1] R. Chen, X. Cheng, D. W. Mitchell, S. A. Hofstadler, Q. Wu, A. L. Rockwood, M. G. Sherman, R. D. Smith. Trapping, detection, and mass determination of coliphage T4 DNA ions of 10^8 Da by electrospray ionization Fourier transform ion cyclotron resonance mass spectrometry. *Anal. Chem.* **1995**, *67*, 1159.

[2] J. J. Gorman, B. L. Furguson, D. Speelman, J. Mills. Determination of the disulfide bond arrangement of human respiratory syncytial virus attachment (G) protein by matrix-assisted laser desorption/ionization time-of-flight mass spectrometry. *Protein Sci.* **1997**, *6*, 1308.

[3] E. P. Go, W. R. Wikoff, Z. Shen, G. O'Maille, H. Morita, T. P. Conrads, A. Nordstrom, S. A. Trauger, W. Uritboonthai, D. A. Lucas, K. C. Chan, T. D. Veenstra, H. Lewicki, M. B. Oldstone, A. Schneemann, G. Siuzdak. Mass spectrometry reveals specific and global molecular transformations during viral infection. *J. Proteome Res.* **2006**, *5*, 2405.

[4] B. Bothner, X. Fan Dong, L. Bibbs, J. E. Johnson, G. Siuzdak. Evidence of viral capsid dynamics using limited proteolysis and mass spectrometry. *J. Biol. Chem.* **1998**, *273*, 673.

[5] D. A. Shepherd, K. Holmes, D. J. Rowlands, N. J. Stonehouse, A. E. Ashcroft. Using ion mobility spectrometry mass spectrometry to decipher the conformational and assembly characteristics of the hepatitis B capsid protein. *Biophys. J.* **2013**, *105*, 1258.

[6] C. G. Alexander, M. C. Jürgens, D. A. Shepherd, S. M. V. Freund, A. E. Ashcroft, N. Ferguson. Thermodynamic origins of protein folding, allostery, and capsid formation in the human hepatitis B virus core protein. *Proc. Natl. Acad. Sci.* **2013**, *110*, E2782.

[7] I. S. Gilmore, M. P. Seah. Ion detection efficiency in SIMS: Dependencies on energy, mass and composition for microchannel plates used in mass spectrometry. *Int. J. Mass Spectrom.* **2000**, *202*, 217.

[8] M. A. Tito, K. Tars, K. Valegard, J. Hajdu, C. V. Robinson. Electrospray time-of-flight mass spectrometry of the intact MS2 virus capsid. *J. Am. Chem. Soc.* **2000**, *122*, 3550.

[9] C. Uetrecht, C. Versluis, N. R. Watts, W. H. Roos, G. J. L. Wuite, P. T. Wingfield, A. C. Steven, A. J. R. Heck. High-resolution mass spectrometry of viral assemblies: Molecular composition and stability of dimorphic hepatitis B virus capsids. *Proc. Natl. Acad. Sci. USA* **2008**, *105*, 9216.

[10] J. Snijder, R. J. Rose, D. Veesler, J. E. Johnson, A. J. R. Heck. Studying 18 MDa virus assemblies with native mass spectrometry. *Angew. Chem. Int. Ed.* **2013**, *52*, 4020.

[11] S. D. Fuerstenau, W. H. Benner. Molecular weight determination of megadalton DNA electrospray ions using charge detection time-of-flight mass spectrometry. *Rapid Commun. Mass Spectrom.* **1995**, *9*, 1528.

[12] W. H. Benner. A gated electrostatic ion trap to repetitiously measure the charge and m/z of large electrospray ions. *Anal. Chem.* **1997**, *69*, 4162.

[13] J. C. Schultz, C. A. Hack, W. H. Benner. Mass determination of megadalton-DNA electrospray ions using charge detection mass spectrometry. *J. Am. Soc. Mass. Spectrom.* **1998**, *9*, 305.

[14] J. C. Schultz, C. A. Hack, W. H. Benner. Polymerase chain reaction products analyzed by charge detection mass spectrometry. *Rapid Commun. Mass Spectrom.* **1999**, *13*, 15.

[15] M. Gamero-Castano. Induction charge detector with multiple sensing stages. *Rev. Sci. Instrum.* **2007**, *78*, 043301.

[16] S. D. Fuerstenau, W. H. Benner, J. J. Thomas, C. Brugidou, B. Bothner, G. Siuzdak. Mass spectrometry of an intact virus. *Angew. Chem. Int. Ed.* **2001**, *40*, 541.

[17] N. C. Contino, M. F. Jarrold. Charge detection mass spectrometry for single ions with a limit of detection of 30 charges. *Int. J. Mass Spectrom.* **2013**, *345/347*, 153.

[18] N. Contino, E. Pierson, D. Keifer, M. Jarrold. Charge detection mass spectrometry with resolved charge states. *J. Am. Soc. Mass Spectrom.* **2013**, *24*, 101.

[19] E. E. Pierson, D. Z. Keifer, N. C. Contino, M. F. Jarrold. Probing higher order multimers of pyruvate kinase with charge detection mass spectrometry. *Int. J. Mass Spectrom.* **2013**, *337*, 50.

[20] H. T. Schmidt, H. Cederquist, J. Jensen, A. Fardi. Conetrap: A compact electrostatic ion trap. *Nucl. Instrum. Methods B* **2001**, *173*, 523.

[21] S. C. J. King. Catalytic head assembling protein in virus morphogenesis. *Nature* **1974**, *251*, 112.

[22] K. Eppler, E. Wyckoff, J. Goates, R. Parr, S. Casjens. Nucleotide sequence of the bacteriophage P22 genes required for DNA packaging. *Virology* **1991**, *183*, 519.

[23] C. M. Teschke, A. McGough, P. A. Thuman-Commike. Penton release from P22 heat expanded capsids suggests importance of stabilizing penton-hexon interactions during capsid maturation. *Biophys. J.* **2003**, *84*, 2585.

[24] P. A. Thuman-Commike, B. Greene, J. A. Malinski, M. Burbea, A. McGough, W. Chiu, P. E. Prevelige. Mechanism of scaffolding-directed virus assembly suggested by comparison of scaffolding-containing and scaffolding-lacking P22 procapsids. *Biophys. J.* **1999**, *76*, 3267.

[25] P. E. Prevelige, D. Thomas, J. King. Scaffolding protein regulates the polymerization of P22 coat subunits into icosahedral shells in vitro. *J. Mol. Biol.* **1988**, *202*, 743.

[26] L. Konermann, E. Ahadi, A. D. Rodriguez, S. Vahidi. Unraveling the mechanism of electrospray ionization. *Anal. Chem.* **2012**, *85*, 2.

[27] J. Fernandez de la Mora. Electrospray ionization of large multiply charged species proceeds via Dole's charged residue mechanism. *Anal. Chim. Acta* **2000**, *406*, 93.

[28] A. J. R. Heck, R. H. H. van den Heuvel. Investigation of intact protein complexes by mass spectrometry. *Mass Spectrom. Rev.* **2004**, *23*, 368.

[29] P. Kebarle, U. H. Verkerk. Electrospray: From ions in solution to ions in the gas phase, what we know now. *Mass Spectrom. Rev.* **2009**, *28*, 898.

[30] K. B. Shelimov, D. E. Clemmer, R. R. Hudgins, M. F. Jarrold. Protein structure in vacuo: Gas-phase conformations of BPTI and cytochrome c. *J. Am. Chem. Soc.* **1997**, *119*, 2240.